Identification of a novel cationic glycolipid in *Streptococcus agalactiae* that contributes to brain entry and meningitis

Luke R. Joyce[a,b], Haider S. Manzer[b], Jéssica da C. Mendonça[b,c], Ricardo Villarreal[b], Prescilla E. Nagao[c] , Kelly S. Doran[b#,] Kelli L. Palmer[a#], and Ziqiang Guan[d#]

[a]Department of Biological Sciences, The University of Texas at Dallas, Richardson, TX, 75080

[b]Department of Immunology and Microbiology, University of Colorado School of Medicine, Aurora, CO, 80045

[c]Rio de Janeiro State University, Roberto Alcântara Gomes Biology Institute, Rio de Janeiro, RJ, Brazil

[d]Department of Biochemistry, Duke University Medical Center, Durham, NC, 27710

Short title: GBS MprF synthesizes a novel glycolipid that contributes to meningitis

#Corresponding authors

Kelly S. Doran: Kelly.Doran@CUAnschutz.edu

Kelli L. Palmer: Kelli.Palmer@UTDallas.edu

Ziqiang Guan: Ziqiang.Guan@Duke.edu

Keywords: Group B *Streptococcus*, Lipidomics, Glycolipid, Meningitis, MprF

Abstract

Bacterial membrane lipids are critical for membrane bilayer formation, cell division, protein localization, stress responses, and pathogenesis. Despite their critical roles, membrane lipids have not been fully elucidated for many pathogens. Here, we report the discovery of a novel cationic glycolipid, Lysyl-Glucosyl-Diacylglycerol (Lys-Glc-DAG) that is synthesized in high abundance by the bacterium *Streptococcus agalactiae* (Group B *Streptococcus*, GBS). To our knowledge, Lys-Glc-DAG is more positively charged than any other known lipids. Lys-Glc-DAG carries two positive net charges per molecule, distinct from the widely described lysylated phospholipid Lysyl-phosphatidylglycerol (Lys-PG) which carries one positive net charge due to the presence of a negatively charged phosphate moiety. We use normal phase liquid chromatography (NPLC) coupled with electrospray ionization (ESI) high-resolution tandem mass spectrometry (HRMS/MS) and genetic approaches to determine that Lys-Glc-DAG is synthesized by the enzyme MprF in GBS, which covalently modifies the neutral glycolipid Glc-DAG with the cationic amino acid lysine. GBS is a leading cause of neonatal meningitis, which requires traversal of the endothelial blood-brain barrier (BBB). We demonstrate that GBS strains lacking *mprF* exhibit a significant decrease in the ability to invade BBB endothelial cells. Further, mice challenged with a GBS∆*mprF* mutant developed bacteremia comparably to Wild-Type infected mice yet had less recovered bacteria from brain tissue and a lower incidence of meningitis. Thus, our data suggest that Lys-Glc-DAG may contribute to bacterial uptake into host cells and disease progression. Importantly, our discovery provides a platform for further study of cationic lipids at the host-pathogen interface.

Introduction

Bacterial cellular membranes are dynamic structures that are critical for survival under varying environmental conditions and are essential for host-pathogen interactions. Phospholipids and glycolipids within the membrane have varying chemical properties that alter the physiology of the membrane, which bacteria can modulate in response to environmental stresses such as pH (1), antibiotic treatment (2), and human metabolites (3). Despite their critical roles in the survival and pathogenesis, membrane lipids have not been carefully characterized using modern lipidomic techniques for many important human pathogens, including *Streptococcus agalactiae* (Group B *Streptococcus*; GBS). GBS colonizes the lower genital and gastrointestinal tracts of ~30% of healthy women (4, 5). However, GBS can cause sepsis and pneumonia in newborns and is a leading cause of neonatal meningitis, resulting in long-lasting neurological effects in survivors (6-8). Due to the severity of the resulting diseases, intrapartum antibiotic prophylaxis is prescribed for colonized pregnant women (7, 9). Even with these measures, a more complete understanding of GBS pathogenesis and new therapeutic and preventive measures are needed to mitigate the devastating impact of GBS neonatal infection.

Research on the pathogenesis of the GBS has mainly focused on cell wall-anchored or secreted proteins and polysaccharides that aid in the attachment to and invasion of host cells. The numerous attachment and virulence factors possessed by the GBS are summarized in a recent review by Armistead *et al* 2019 (10). Comparatively little is known about GBS cellular membrane lipids. To our knowledge, the only characterization of GBS lipids prior to our current study was the identification of the phospholipids

70 phosphatidylglycerol (PG), cardiolipin (CL), and lysyl-phosphatidylglycerol (Lys-PG) in
71 GBS (11-13). Similarly, investigation into the glycolipids of the GBS membrane has
72 focused on di-glucosyl-diacylglycerol (Glc_2-DAG), which is the lipid anchor of the Type I
73 lipoteichoic acid, and its role in pathogenesis (14).
74
75 In this study, we utilized normal phase liquid chromatography (NPLC) coupled with
76 electrospray ionization (ESI) high-resolution tandem mass spectrometry (HRMS/MS) to
77 characterize the GBS membrane lipid composition, and identified a novel cationic
78 glycolipid, lysyl-glucosyl-diacylglycerol (Lys-Glc-DAG), which comprises a major portion
79 of the GBS total lipid extract. While Lys-PG has been reported in a range of bacterial
80 species (15), Lys-Glc-DAG represents, to our knowledge, the first example of lysine
81 modification of a neutral glycolipid. By gene deletion and heterologous expression, we
82 show the GBS MprF enzyme is responsible for the biosynthesis of both the novel Lys-
83 Glc-DAG and Lys-PG. Most strikingly, using an *in vivo* hematogenous murine infection
84 model, we demonstrate that MprF does not contribute to GBS bloodstream survival. This
85 distinguishes the GBS MprF from the well-known *Staphylococcus aureus* MprF, which
86 synthesizes only Lys-PG (16, 17). Rather, GBS MprF contributes specifically to meningitis
87 and penetration of the blood-brain barrier. These results greatly expand our knowledge
88 of naturally occurring lipids and MprF functionality and reveal insights into the
89 pathogenesis of meningitis caused by GBS.
90
91 **Results**
92 **Identification of Lys-Glc-DAG, a novel cationic glycolipid in GBS**

The membrane lipids of three GBS clinical isolates of representative serotypes were characterized: COH1 (18), A909 (19), CNCTC 10/84 and CJB111 (20) (serotypes III, 1a, and V, respectively). Common Gram-positive bacterial lipids were identified by normal phase LC coupled with negative ion ESI/MS/MS, including diacylglycerol (DAG), monohexosyldiacylglycerol (MHDAG), dihexosyldiacylglycerol (DHDAG), phosphatidylglycerol (PG), and lysyl-phosphatidylglycerol (Lys-PG), as shown by the negative total ion chromatogram (TIC) (Fig. 1A).

Surprisingly, the positive TIC (Fig. 1B, S1 Fig) shows highly abundant peaks of unknown identity at the retention time ~25-29 min. The mass spectra (Fig. 1C) and LC retention times of this lipid do not match with any other bacterial lipids we have analyzed or exact masses in lipidomic databases (21, 22). Tandem MS (MS/MS) in the positive ion mode (Fig. 1D), negative ion mode (Fig. 1E), and high-resolution mass measurement (Fig. 1C) allowed us to propose lysyl-glucosyl-diacylglycerol (Lys-Glc-DAG) (Fig. 1F) as the structure of this unknown lipid. Observed and exact masses of Lys-Glc-DAG are shown in S1 Table. The assignment of glucose was based on the observation that glucosyl-diacylglycerol (Glc-DAG) is a major membrane component of GBS and other streptococci (14), and results from an isotopic labeling experiment using ^{13}C-labeled glucose (Glucose-$^{13}C_6$). The assignment of lysine modification was supported by an isotopic labeling experiment with deuterated lysine (lysine-*d4*). The expected mass shifts (+4 Da) were observed in both molecular ions and MS/MS product ions (S2 Fig). Comparison of both MS/MS spectra of labeled (Glucose-$^{13}C_6$) and unlabeled Lys-Glc-DAG indicates the lysine residue is linked to the 6-position of glucose (S2 Fig). Lys-Glc-DAG consists of

116 several molecular species with different fatty acyl compositions resulting in different
117 retention times and multiple, unresolved TIC peaks (~25-29 min).
118
119 **GBS MprF synthesizes Lys-Glc-DAG**
120 The enzyme MprF (multiple peptide resistance factor) catalyzes the aminoacylation of PG
121 with lysine in some Gram-positive pathogens (16, 23). We determined that GBS MprF is
122 responsible and sufficient for synthesizing Lys-Glc-DAG as well as Lys-PG. Deletion of
123 *mprF* from both COH1 and CJB111 abolishes Lys-Glc-DAG and Lys-PG synthesis, which
124 are restored by complementation (Fig. 1G, S3 Fig). Deletion of GBS *mprF* does not confer
125 a growth defect in Todd-Hewitt broth or tissue culture medium. The oral colonizer
126 *Streptococcus mitis* does not encode *mprF* or synthesize Lys-PG but synthesizes Glc-
127 DAG and PG (2, 3). Heterologous expression of GBS *mprF* in *S. mitis* results in Lys-Glc-
128 DAG and Lys-PG production (Fig. 1H), while expression of *Enterococcus faecium mprF*
129 results in only Lys-PG production (Fig. 1H), as expected (1). Biosynthetic pathways
130 involving MprF are shown in Fig. 1I.
131
132 **MprF contributes to GBS pathogenesis**
133 We investigated whether MprF contributes to GBS invasion into brain endothelial cells
134 and development of meningitis. To mimic the human blood-brain barrier (BBB), we utilized
135 the human cerebral microvascular endothelial cell line hCMEC/D3. *In vitro* assays for
136 adhesion and invasion were performed as described previously (14, 24, 25). There was
137 no significant difference in the ability of Δ*mprF* compared to WT and complement cells to
138 attach to hCMEC/D3 cells (Fig. 2A). However, we observed a significant decrease in the

amount of Δ*mprF* recovered from the intracellular compartment of hCMEC/D3 cells (Fig. 2A). The reduced invasion phenotype was confirmed in the hypervirulent serotype V strain, CJB111 (26, 27) (S4 Fig). Intracellular survival requires GBS to survive low pH conditions in lysosomes (pH 4.5 – 5.5) (28), and Δ*mprF* is unable to survive low pH conditions (Fig. 2B). This suggests that MprF promotes GBS invasion and possibly intracellular survival in brain endothelial cells.

We hypothesized that these *in vitro* phenotypes of Δ*mprF* would translate into a diminished ability to penetrate the BBB and produce meningitis *in vivo*. Using our standard model of GBS hematogenous meningitis (14, 24) mice were challenged with either WT GBS or Δ*mprF*. Mice were sacrificed at 72 h to determine bacterial loads in blood, lung and brain tissue. We recovered significantly less CFU in the brains of Δ*mprF*-infected mice compared to the WT-infected mice (Fig. 2C). However, there was no significant difference in CFU recovered from the bloodstream or the lung (Fig. 2D,E), demonstrating that Δ*mprF* does not have a general defect in bloodstream survival or tissue invasion *in vivo*. Furthermore, mice challenged with WT GBS had significantly more meningeal thickening and neutrophil chemokine, KC, in brain homogenates compared to Δ*mprF* mutant-infected animals (Fig. 2F-H). Taken together, *mprF* contributes to GBS penetration into the brain and to the pathogenesis of meningitis *in vivo*.

Discussion

Here, we report that GBS MprF uniquely synthesizes a novel cationic glycolipid Lys-Glc-DAG in high abundance plays a role in the invasion of human endothelial cells. This work

establishes that GBS capitalizes on MprF to modulate charges of both glycolipids and phospholipids at the membrane, which is unprecedented

Previously MprF has been shown to catalyze the aminoacylation of the anionic phospholipid PG in a range of Gram-positive and Gram-negative bacteria (16, 23). MprF is a membrane-bound enzyme comprised of a N-terminal lipid flippase domain (29) and a C-terminal catalytic domain that catalyzes the aminoacylation of the glycerol group of PG by using aminoacyl-tRNAs as the amino acid donors (30-32). An important function of PG aminoacylation is proposed to decrease the net negative charge of the cellular envelope to confer protection from cationic antimicrobial peptides (CAMPs) produced by host immune systems and bacteriocins produced by competitor bacteria (16, 23). However, a previous study observed no contribution of *mprF* to GBS *in vitro* susceptibility to commonly studied CAMPs, which is unlike the well-characterized *S. aureus mprF* (33), thus highlighting the unique differences between the extracellular surface of these bacteria.

Based on our tissue culture and mouse infection experiments, we propose that GBS have an MprF enzyme and corresponding cellular lipid properties that are adapted for efficient invasion of mammalian cells. Deletion of *mprF* impacts the ability of GBS to enter the brain and promote meningitis *in vivo*. This suggests that MprF plays a role in BBB penetration and not invasion into the lung, however additional studies are warranted to examine other tissue sites. It is unknown how lysinylated lipids in the GBS membrane, which is covered by a layer of peptidoglycan, mechanistically impact invasion. Because

Lys-Glc-DAG is abundantly synthesized by GBS MprF, with Lys-PG a comparatively minor product, it is likely that Lys-Glc-DAG is the most relevant lipid for meningitis pathogenesis. Speculatively, Lys-Glc-DAG may contribute to membrane vesicle (MV) formation by GBS. MVs have previously been shown to be pro-inflammatory and result in preterm birth and fetal death in mice (34), but have not been studied during meningitis progression. In future studies, it will be key to investigate this, as well as the specific host inflammatory and signaling responses to the GBS *mprF* mutant.

Our identification of the novel Lys-Glc-DAG glycolipid rationalizes further study of the lipidomes of human pathogens. First, lipids contribute to virulence, and understanding these virulence mechanisms and the mechanisms for lipid synthesis may identify novel antimicrobial drug targets. The decreased *in vivo* pathogenicity of the Δ*mprF* mutant identifies GBS MprF as a candidate for targeting by antimicrobial strategies. Moreover, Lys-Glc-DAG could be utilized as a specific molecular biomarker for GBS diagnostics. In addition, engineered cationic lipids are utilized in lipid nanoparticles for mRNA vaccine and drug delivery and are required for uptake of particles into cells (35, 36). Substantial effort has been dedicated to the synthesis of cationic lipids with low toxicity and efficient delivery properties. Lys-Glc-DAG is a naturally occurring, strongly cationic lipid with potential for use in lipid nanoparticles for vaccine and drug delivery. Importantly, our discovery suggests that lipidome analysis of human pathogens is likely to reveal novel lipids of biotechnological utility.

Materials and methods

208 **Bacterial strains, media, and growth conditions**

209 See S2 Table for strains used in this study. GBS strains were grown statically at 37°C in
210 Todd-Hewitt Broth (THB) and *S. mitis* strains were grown statically at 37°C and 5% CO_2,
211 unless otherwise stated. Streptococcal chemically defined medium (37) was diluted from
212 stock as described (38) with 1% w/v glucose (referred to as DM), slightly modified from
213 (39), unless otherwise stated. *Escherichia coli* strains were grown in Lysogeny Broth (LB)
214 at 37°C with rotation at 225 rpm. Kanamycin and erythromycin (Sigma-Aldrich) were
215 supplemented to media at 50 µg/mL and 300 µg/mL for *E. coli,* respectively, or 300 µg/mL
216 and 5 µg/mL, respectively, for streptococcal strains.

217

218 **Routine molecular biology techniques**

219 All PCR reactions utilized Phusion polymerase (Thermo Fisher). PCR products and
220 restriction digest products were purified using GeneJET PCR purification kit (Thermo
221 Fisher) per manufacturer protocols. See S3 Table for primers. Plasmids were extracted
222 using GeneJET plasmid miniprep kit (Thermo Fisher) per manufacturer protocols.
223 Restriction enzyme digests utilized XbaI, XhoI, and PstI (New England Biolabs) for 3 h at
224 37°C in a water bath. Ligations utilized T4 DNA ligase (New England Biolabs) at 16°C
225 overnight or Gibson Assembly Master Mix (New England Biolabs) per manufacturer
226 protocols where stated. All plasmid constructs were sequence confirmed by Sanger
227 sequencing (Massachusetts General Hospital DNA Core or CU Anschutz Molecular
228 Biology Core).

229

230 **Deuterated lysine and $^{13}C_6$-D-glucose isotope tracking**

A GBS COH1 colony was inoculated into 15 mL of DM containing 450 µM lysine-*d4* (Cambridge Isotopes Laboratories) or a single COH1 colony was inoculated into 10 mL DM supplemented with 0.5% w/v $^{13}C_6$D-glucose (U-13C6, Cambridge Isotopes Laboratories) for overnight growth for lipidomic analysis described below.

Construction of MprF expression plasmids

Genomic DNA was isolated using the Qiagen DNeasy Blood and Tissue kit per the manufacturer's protocol with the exception that cells were pre-treated with 180 µL 50 mg/mL lysozyme, 25 µL 2500 U/mL mutanolysin, and 15 µL 20 mg/mL pre-boiled RNase A and incubated at 37°C for 2 h. The *mprF* genes from GBS COH1, (GBSCOH1_1931), GBS CJB111 (ID870_10050), and *E. faecium* 1,231,410 (EFTG_00601) were amplified and either Gibson ligated into pABG5Δ*phoZ* (40) or ligated into pDCErm (41). Plasmid constructs were transformed into chemical competent *E. coli*. Briefly, chemically competent cells were incubated for 10 min on ice with 5 µL of Gibson reaction before heat shock at 42°C for 70 sec, then placed on ice for 2 min before 900 µL of cold SOC medium was added. Outgrowth was performed at 37°C, with shaking at 225 rpm, for 1 h. Cultures were plated on LB agar plates containing 50 µg/mL kanamycin. Colonies were screened by PCR for presence of the *mprF* insert.

Expression of *mprF* in *S. mitis*

Natural transformation was performed as previously described (3). Briefly, precultures were thawed at room temperature, diluted in 900 µL of THB, further diluted 1:50 in prewarmed 5 mL THB, and incubated for 45 min at 37°C. 500 µL of culture was then

aliquoted with 1 µL of 1 mg/ml competence-stimulating peptide (EIRQTHNIFFNFFKRR) and 1 µg/mL plasmid. Transformation reaction mixtures were cultured for 2 h at 37°C in microcentrifuge tubes before being plated on THB agar supplemented with 300 µg/mL kanamycin. Single transformant colonies were cultured in 15 mL THB overnight. PCR was used to confirm the presence of the *mprF* insert on the plasmid. Plasmids were extracted and sequence confirmed as described above. Lipidomics was performed as described below in biological triplicate.

Construction of *mprF* deletion plasmids

Regions ~2 kb upstream and downstream of the GBS COH1 *mprF* (GBSCOH1_1931) or CJB111 (ID870_10050) were amplified using PCR. Plasmid, pMBSacB (42), and the PCR products were digested using appropriate restriction enzymes and ligated overnight. 7 µL of the ligation reaction was transformed into chemically competent *E. coli* DH5α as described above, except that outgrowth was performed at 28°C with shaking at 225 rpm for 90 min prior to plating on LB agar supplemented with 300 µg/mL erythromycin. Plates were incubated at 28°C for 72 h. Colonies were screened by PCR for correct plasmid construction. Positive colonies were inoculated into 50 mL LB media containing antibiotic and incubated at 28°C with rotation at 225 rpm for 72 h. Cultures were pelleted using a Sorvall RC6+ centrifuge at 4,280 x *g* for 6 min at room temperature. Plasmid was extracted as described above except the cell pellet was split into 5 columns to prevent overloading and serial eluted into 50 µL. Plasmid construction was confirmed via restriction digest using XhoI and XbaI, and the insert was PCR amplified and sequence-verified.

277

278 **Generation of electrocompetent GBS cells for *mprF* knockout**

279 Electrocompetent cells were generated as described (42) with minor modifications.
280 Briefly, a GBS COH1 or CJB111 colony was inoculated in 5 mL M17 medium (BD Bacto)
281 with 0.5% glucose and grown overnight at 37°C. The 5 mL was used to inoculate a second
282 overnight culture of 50 mL pre-warmed filter-sterilized M17 medium containing 0.5%
283 glucose, 0.6% glycine, and 25% PEG 8000. The second overnight was added to 130 mL
284 of the same medium and grown for 1 h at 37°C. Cells were pelleted at 3,200 x *g* in a
285 Sorvall RC6+ at 4°C for 10 min. Cells were washed twice with 25 mL cold filter-sterilized
286 GBS wash buffer containing 25% PEG 8000 and 10% glycerol in water, and pelleted as
287 above. Cell pellets were re-suspended in 1 mL GBS wash buffer and either used
288 immediately for transformation or stored in 100 µL aliquots at -80°C until use.

289

290 **Deletion of GBS COH1 and CJB111 *mprF***

291 Electrocompetent cells were generated as described (42) with minor modifications. The
292 double crossover homologous recombination knockout strategy was performed as
293 described previously (25, 42, 43) with minor modifications. 1 µg of plasmid was added to
294 electrocompetent GBS cells and transferred to a cold 1 mm cuvette (Fisher or BioRad).
295 Electroporation was carried out at 2.5 kV on an Eppendorf eporator. 1 mL of THB
296 containing 12.5% PEG 8000, 20 mM $MgCl_2$, and 2 mM $CaCl_2$ was immediately added
297 and then the entire reaction was transferred to a glass culture tube. Outgrowth was at
298 28°C for 2 h followed by plating on THB agar supplemented with 5 µg/mL erythromycin.
299 Plates were incubated for 48 h at 28°C. A single colony was cultured overnight in 5 mL

300 THB with 5 µg/mL erythromycin at 28°C. The culture was screened via PCR for the
301 plasmid insert with the initial denaturing step extended to 10 min. The overnight culture
302 was diluted 1:1000 THB containing 5 µg/mL erythromycin and incubated overnight at
303 37°C to promote single cross over events. The culture was then serial diluted and plated
304 on THB agar plates with antibiotic and incubated at 37°C overnight. Colonies were
305 screened for single crossover events by PCR. Single crossover colonies were inoculated
306 in 5 mL THB at 28°C to promote double crossover events. Overnight cultures were diluted
307 1:1000 into 5 mL THB containing sterile 0.75 M sucrose and incubated at 37°C. Overnight
308 cultures were serial diluted and plated on THB agar and incubated at 37°C overnight.
309 Colonies were patched onto THB agar with and without 5 µg/mL erythromycin to confirm
310 loss of plasmid. Colonies were also screened by PCR for the loss of *mprF*. Colonies
311 positive for the loss of *mprF* were inoculated into 5 mL THB at 37°C. Cultures were
312 stocked and gDNA extracted as described above, with minor modifications. Sequence
313 confirmation of the *mprF* knockout was done via Sanger sequencing (Massachusetts
314 General Hospital DNA Core or CU Anschutz Molecular Biology Core). The mutant was
315 grown overnight in 15 mL THB at 37°C and pelleted at 6,150 x *g* for 5 min in a Sorvall
316 RC6+ centrifuge at room temperature for lipid extraction as described. Genomic DNA of
317 COH1Δ*mprF* was isolated as described above and whole genome sequencing was
318 performed in paired-end reads (2 by 150 bp) on the Illumina NextSeq 550 platform at the
319 Microbial Genome Sequencing Center (Pittsburgh, PA). Illumina sequence reads are
320 deposited in the Sequence Read Archive, accession PRJNA675025.
321
322 **Complementation of *mprF* in COH1Δ*mprF* and CJB111Δ*mprF***

Electrocompetent GBS strains were generated as previously described (44). Briefly, GBSΔ*mprF* was inoculated into 5 mL THB with 0.6% glycine and grown overnight. The culture was expanded to 50 mL in pre-warmed THB with 0.6% glycine and grown to an OD_{600} nm of 0.3 and pelleted for 10 min at 3200 x *g* at 4°C in a Sorvall RC6+ floor centrifuge. The pellet was kept on ice through the remainder of the protocol. The pellet was washed twice with 25 mL and once with 10 mL of cold 0.625 M sucrose and pelleted as above. The cell pellet was resuspended in 400 µL of cold 20% glycerol, aliquoted in 50 µL aliquots, and used immediately or stored at -80°C until use. Electroporation was performed as described above, with recovery in THB supplemented with 0.25 M sucrose, and plated on THB agar with kanamycin at 300 µg/mL.

Acidic Bligh-Dyer extractions

Centrifugation was performed using a Sorvall RC6+ centrifuge. Cultures were pelleted at 4,280 x *g* for 5 min at room temperature unless otherwise stated. The supernatants were removed, and cell pellets were stored at -80°C until acidic Bligh-Dyer lipid extractions were performed as described (3). Briefly, cell pellets were resuspended in 1X PBS (Sigma-Aldrich) and transferred to Coring Pyrex glass tubes with PTFR-lined caps (VWR), followed by 1:2 vol:vol chloroform:methanol addition. Single phase extractions were vortexed periodically and incubated at room temperature for 15 minutes before 500 x *g* centrifugation for 10 min. A two-phase Bligh-Dyer was achieved by addition of 100 µL 37% HCl, 1 mL $CHCl_3$, and 900 µl of 1X PBS, which was then vortexed and centrifuged for 5 min at 500 x *g.* The lower phase was removed to a new tube and dried under nitrogen before being stored at -80°C prior to lipidomic analysis.

346

347 **Liquid Chromatography/Electrospray Ionization Mass Spectrometry**

348 Normal phase LC was performed on an Agilent 1200 quaternary LC system equipped
349 with an Ascentis silica HPLC column (5 µm; 25 cm by 2.1 mm; Sigma-Aldrich) as
350 described previously (45, 46). Briefly, mobile phase A consisted of chloroform-methanol-
351 aqueous ammonium hydroxide (800:195:5, vol/vol), mobile phase B consisted of
352 chloroform-methanol-water-aqueous ammonium hydroxide (600:340:50:5, vol/vol), and
353 mobile phase C consisted of chloroform-methanol-water-aqueous ammonium hydroxide
354 (450:450:95:5, vol/vol). The elution program consisted of the following: 100% mobile
355 phase A was held isocratically for 2 min, then linearly increased to 100% mobile phase B
356 over 14 min, and held at 100% mobile phase B for 11 min. The LC gradient was then
357 changed to 100% mobile phase C over 3 min, held at 100% mobile phase C for 3 min,
358 and, finally, returned to 100% mobile phase A over 0.5 min and held at 100% mobile
359 phase A for 5 min. The LC eluent (with a total flow rate of 300 µl/min) was introduced into
360 the ESI source of a high-resolution TripleTOF5600 mass spectrometer (Sciex,
361 Framingham, MA). Instrumental settings for negative-ion ESI and MS/MS analysis of lipid
362 species were: IS = -4,500 V, CUR = 20 psi, GSI = 20 psi, DP = -55 V, and FP = -150V.
363 Settings for positive-ion ESI and MS/MS analysis were: IS = +5,000 V, CUR = 20 psi, GSI
364 = 20 psi, DP = +55 V, and FP = +50V. The MS/MS analysis used nitrogen as the collision
365 gas. Data analysis was performed using Analyst TF1.5 software (Sciex, Framingham,
366 MA).

367

368 **pH-adjusted THB growth**

Approximately 30 mL of fresh THB were adjusted to different pH values, measured using a Mettler Toledo FiveEasy pH/MV meter, and sterile-filtered using 0.22 µM syringe filters. A final volume of 200 µL culture medium was aliquoted per well in a flat-bottom 96 well plate (Falcon); culture media were not supplemented with antibiotics. Overnight cultures of GBS strains were used to inoculate the wells to a starting OD_{600nm} 0.02 per well. Plates were incubated for 24 h at 37°C before OD_{600nm} was read using a BioTek MX Synergy 2 plate reader. This experiment was performed in biological triplicate.

hCMEC cell adherence and invasion assays

Human Cerebral Microvascular Endothelial cells hCMEC/D3 (obtained from Millipore) were grown in EndoGRO-MV complete media (Millipore, SCME004) supplemented with 5% fetal bovine serum (FBS) and 1 ng/ml fibroblast growth factor-2 (FGF-2; Millipore). Cells were grown in tissue culture treated 24 well plates and 5% CO_2 at 37°C.

Assays to determine the total number of bacteria adhered to host cells or intracellular bacteria were performed as described previously (24, 25). Briefly, bacteria were grown to mid log phase (OD_{600nm} 0.4-0.5) and normalized to 1 x 10^8 to infect cell monolayers at a multiplicity of infection (MOI) of 1 (1 x 10^5 CFU per well). The total cell-associated GBS were recovered after 30 min incubation. Cells were washed slowly five times with 500 µL 1X PBS (Sigma) and detached by addition of 100 µL of 0.25% trypsin-EDTA solution (Gibco) and incubation for 5 min before lysing the eukaryotic cells with the addition of 400 µL of 0.025% Triton X-100 (Sigma) and vigorous pipetting. The lysates were then serially diluted and plated on THB agar and incubated overnight to determine CFU. Bacterial

invasion assays were performed as described above except infection plates were incubated for 2 h before incubation with 100 µg gentamicin (Sigma) and 5 µg penicillin (Sigma) supplemented media for an additional 2 h to kill all extracellular bacteria, prior to being trypsinized, lysed, and plated as described. Experiments were performed in biological triplicate with four technical replicates per experiment.

Murine model of GBS hematogenous meningitis

All animal experiments were conducted under the approval of the Institutional Animal Care and Use Committee (#00316) at the University of Colorado Anschutz Medical Campus and performed using accepted veterinary standards. The murine meningitis model was performed as previously described (25, 47, 48). Briefly, 7-week-old male CD1 (Charles River) mice were challenged intravenously with 1×10^9 CFU of WT COH1 or the isogenic Δ*mprF* mutant. At 72 h post-infection, mice were euthanized and blood, lung and brain tissue were harvested, homogenized, and serially diluted on THB agar plates to determine bacterial CFU.

Histology and ELISA

Mouse brain tissue was frozen in OCT compound (Sakura) and sectioned using a CM1950 cryostat (Leica). Sections were stained using hematoxylin and eosin (Sigma) and images were taken using a BZ-X710 microscope (Keyence). Images were analyzed using ImageJ software. Meningeal thickening was quantified from sections taken from three different mice per group, and six images per slide. Meningeal thickening was quantified across two points per image. KC protein from mouse brain homogenates was

415 detected by enzyme-linked immunosorbent assay according to the manufacturer's
416 instructions (R&D systems).
417
418 **Ethics Statement**
419 Animal experiments were approved by the Institutional Animal Care and Use Committee
420 (IACUC) at University of Colorado Anschutz Medical Campus protocol #00316 and were
421 performed using accepted veterinary standards. The University of Colorado Anschutz
422 Medical Campus is AAALAC accredited; and its facilities meet and adhere to the
423 standards in the "Guide for the Care and Use of Laboratory Animals".
424
425 **Conflict of interest**
426 The authors have declared that no conflict of interest exists.
427
428 **Acknowledgements**
429 We thank Kathryn Patras at the University of California San Diego for the CNCTC 10/84
430 strain and Moutusee Islam in Kelli Palmer's lab at The University of Texas at Dallas for
431 *E. faecium* 1,231,410 DNA.
432
433 The work was supported in part by T32 5T32AI052066-18 and F31 AI164674 for H.S.M,
434 the Coordenação de Aperfeiçoamento de Pessoal de Nível Superior, Brazil (CAPES;
435 finance code 001 to J.D.C.M), by grants R01NS116716 and R01AI153332 from the
436 National Institutes of Health (NIH) to K.S.D and associated NIH/NINDS supplement from
437 R01NS116716 to R.V, NIH grant R21AI130666 and the Cecil H. and Ida Green Chair in

438 Systems Biology Science to K.P, NIH grant R56AI139105 to K.P and Z.G, and NIH grant
439 U54GM069338 to Z.G.

440

441 **References**

442 1. Roy H. Tuning the properties of the bacterial membrane with aminoacylated
443 phosphatidylglycerol. IUBMB Life. 2009;61:940-53.
444 2. Adams HM, Joyce LR, Guan Z, Akins RL, Palmer KL. *Streptococcus mitis* and *S.*
445 *oralis* Lack a Requirement for CdsA, the Enzyme Required for Synthesis of Major
446 Membrane Phospholipids in Bacteria. Antimicrobial agents and chemotherapy.
447 2017;61:e02552-16.
448 3. Joyce LR, Guan Z, Palmer KL. Phosphatidylcholine Biosynthesis in Mitis Group
449 Streptococci via Host Metabolite Scavenging. Journal of bacteriology.
450 2019;201:e00495-19.
451 4. Wilkinson HW. Group B Streptococcal Infection in Humans. Annual Review of
452 Microbiology. 1978;32:41-57.
453 5. Doran KS, Nizet V. Molecular pathogenesis of neonatal Group B Streptococcal
454 infection: No longer in its infancy. Molecular Microbiology. 2004;54:23-31.
455 6. Hall J, Adams NH, Bartlett L, Seale AC, Lamagni T, Bianchi-Jassir F, et al.
456 Maternal Disease With Group B *Streptococcus* and Serotype Distribution Worldwide:
457 Systematic Review and Meta-analyses. Clinical infectious diseases : an official
458 publication of the Infectious Diseases Society of America. 2017;65:S112-S24.
459 7. Schuchat A. Epidemiology of Group B Streptococcal disease in the United
460 States: shifting paradigms. Clinical microbiology reviews. 1998;11:497-513.
461 8. Edwards MS, Rench MA, Haffar AA, Murphy MA, Desmond MM, Baker CJ.
462 Long-term sequelae of Group B Streptococcal meningitis in infants. The Journal of
463 pediatrics. 1985;106:717-22.
464 9. Ohlsson A, Shah VS. Intrapartum antibiotics for known maternal Group B
465 Streptococcal colonization. The Cochrane database of systematic reviews.
466 2014:CD007467.
467 10. Armistead B, Oler E, Adams Waldorf K, Rajagopal L. The Double Life of Group B
468 *Streptococcus*: Asymptomatic Colonizer and Potent Pathogen. Journal of Molecular
469 Biology. 2019;431:2914-31.
470 11. Curtis J, Kim G, Wehr NB, Levine RL. Group B Streptococcal phospholipid
471 causes pulmonary hypertension. Proceedings of the National Academy of Sciences of
472 the United States of America. 2003;100:5087-90.
473 12. Fischer W. The polar lipids of Group B Streptococci. II. Composition and
474 positional distribution of fatty acids. Biochimica et biophysica acta. 1977;487:89-104.
475 13. Joyce LR, Guan Z, Palmer KL. *Streptococcus pneumoniae*, *S. pyogenes* and *S.*
476 *agalactiae* membrane phospholipid remodelling in response to human serum.
477 Microbiology (Reading). 2021;167(5).

14. Doran KS, Engelson EJ, Khosravi A, Maisey HC, Fedtke I, Equils O, et al. Blood-brain barrier invasion by Group B *Streptococcus* depends upon proper cell-surface anchoring of lipoteichoic acid. The Journal of clinical investigation. 2005;115:2499-507.
15. Slavetinsky C, Kuhn S, Peschel A. Bacterial aminoacyl phospholipids - Biosynthesis and role in basic cellular processes and pathogenicity. Biochimica et biophysica acta Molecular and cell biology of lipids. 2017;1862:1310-8.
16. Peschel A, Jack RW, Otto M, Collins LV, Staubitz P, Nicholson G, et al. *Staphylococcus aureus* resistance to human defensins and evasion of neutrophil killing via the novel virulence factor MprF is based on modification of membrane lipids with L-lysine. Journal of Experimental Medicine. 2001;193:1067-76.
17. Weidenmaier C, Peschel A, Kempf VA, Lucindo N, Yeaman MR, Bayer AS. DltABCD- and MprF-mediated cell envelope modifications of *Staphylococcus aureus* confer resistance to platelet microbicidal proteins and contribute to virulence in a rabbit endocarditis model. Infect Immun. 2005;73(12):8033-8.
18. Kuypers JM, Heggen LM, Rubens CE. Molecular analysis of a region of the Group B *Streptococcus* chromosome involved in type III capsule expression. Infection and immunity. 1989;57:3058-65.
19. Lancefield RC, McCarty M, Everly WN. Multiple mouse-protective antibodies directed against Group B Streptococci. Special reference to antibodies effective against protein antigens. The Journal of experimental medicine. 1975;142:165-79.
20. Wilkinson HW. Nontypable Group B Streptococci isolated from human sources. Journal of clinical microbiology. 1977;6:183-4.
21. Smith CA, O'Maille G, Want EJ, Qin C, Trauger SA, Brandon TR, et al. METLIN: a metabolite mass spectral database. Ther Drug Monit. 2005;27(6):747-51.
22. Sud M, Fahy E, Cotter D, Brown A, Dennis EA, Glass CK, et al. LMSD: LIPID MAPS structure database. Nucleic Acids Res. 2007;35(Database issue):D527-32.
23. Roy H, Ibba M. RNA-dependent lipid remodeling by bacterial multiple peptide resistance factors. Proceedings of the National Academy of Sciences of the United States of America. 2008;105:4667-72.
24. Deng L, Spencer BL, Holmes JA, Mu R, Rego S, Weston TA, et al. The Group B Streptococcal surface antigen I/II protein, BspC, interacts with host vimentin to promote adherence to brain endothelium and inflammation during the pathogenesis of meningitis. PLoS pathogens. 2019;15:e1007848.
25. Spencer BL, Deng L, Patras KA, Burcham ZM, Sanches GF, Nagao PE, et al. Cas9 contributes to Group B Streptococcal colonization and disease. Frontiers in Microbiology. 2019;10:1-15.
26. Faralla C, Metruccio MM, De Chiara M, Mu R, Patras KA, Muzzi A, et al. Analysis of two-component systems in Group B *Streptococcus* shows that RgfAC and the novel FspSR modulate virulence and bacterial fitness. mBio. 2014;5(3):e00870-14.
27. Spencer BL, Chatterjee A, Duerkop BA, Baker CJ, Doran KS. Complete Genome Sequence of Neonatal Clinical Group B Streptococcal Isolate CJB111. Microbiology resource announcements. 2021;10.
28. Mu R, Cutting AS, Del Rosario Y, Villarino N, Stewart L, Weston TA, et al. Identification of CiaR Regulated Genes That Promote Group B Streptococcal Virulence and Interaction with Brain Endothelial Cells. PLoS One. 2016;11(4):e0153891.

29. Ernst CM, Kuhn S, Slavetinsky CJ, Krismer BB, Heilbronner S, Gekeler C, et al. The Lipid-Modifying Multiple Peptide Resistance Factor Is an Oligomer Consisting of Distinct Interacting Synthase and Flippase subunits. mBio. 2015;6:1-9.
30. Roy H, Ibba M. Broad range amino acid specificity of RNA-dependent lipid remodeling by multiple peptide resistance factors. Journal of Biological Chemistry. 2009;284:29677-83.
31. Hebecker S, Krausze J, Hasenkampf T, Schneider J, Groenewold M, Reichelt J, et al. Structures of two bacterial resistance factors mediating tRNA-dependent aminoacylation of phosphatidylglycerol with lysine or alanine. Proceedings of the National Academy of Sciences of the United States of America. 2015;112:10691-6.
32. Lennarz WJ, Nesbitt JA, Reiss J. The participation of sRNA in the enzymatic synthesis of O-L-lysyl phosphatidylgylcerol in *Staphylococcus aureus*. Proceedings of the National Academy of Sciences of the United States of America. 1966;55:934-41.
33. Saar-Dover R, Bitler A, Nezer R, Shmuel-Galia L, Firon A, Shimoni E, et al. D-alanylation of lipoteichoic acids confers resistance to cationic peptides in Group B *Streptococcus* by increasing the cell wall density. PLoS pathogens. 2012;8:e1002891.
34. Surve MV, Anil A, Kamath KG, Bhutda S, Sthanam LK, Pradhan A, et al. Membrane Vesicles of Group B *Streptococcus* Disrupt Feto-Maternal Barrier Leading to Preterm Birth. PLOS Pathogens. 2016;12:e1005816.
35. Reichmuth AM, Oberli MA, Jaklenec A, Langer R, Blankschtein D. mRNA vaccine delivery using lipid nanoparticles. Ther Deliv. 2016;7(5):319-34.
36. Hafez IM, Maurer N, Cullis PR. On the mechanism whereby cationic lipids promote intracellular delivery of polynucleic acids. Gene Ther. 2001;8(15):1188-96.
37. Van De Rijn I, Kessler RE. Growth characteristics of Group A Streptococci in a new chemically defined medium. Infection and Immunity. 1980;27:444-8.
38. Chang JC, LaSarre B, Jimenez JC, Aggarwal C, Federle MJ. Two Group A Streptococcal peptide pheromones act through opposing rgg regulators to control biofilm development. PLoS Pathogens. 2011;7:e1002190.
39. Gupta R, Shah P, Swiatlo E. Differential gene expression in *Streptococcus pneumoniae* in response to various iron sources. Microbial Pathogenesis. 2009;47:101-9.
40. Granok AB, Parsonage D, Ross RP, Caparon MG. The RofA binding site in *Streptococcus pyogenes* is utilized in multiple transcriptional pathways. Journal of bacteriology. 2000;182:1529-40.
41. Jeng A, Sakota V, Li Z, Datta V, Beall B, Nizet V. Molecular genetic analysis of a Group A *Streptococcus* operon encoding serum opacity factor and a novel fibronectin-binding protein, SfbX. J Bacteriol. 2003;185(4):1208-17.
42. Hooven TA, Bonakdar M, Chamby AB, Ratner AJ. A Counterselectable Sucrose Sensitivity Marker Permits Efficient and Flexible Mutagenesis in *Streptococcus agalactiae*. Applied and environmental microbiology. 2019;85:1-13.
43. Holo H, Nes IF. High-frequency transformation, by electroporation, of *Lactococcus lactis* subsp. *cremoris* grown with glycine in osmotically stabilized media. Applied and Environmental Microbiology. 1989;55:3119-23.
44. Framson PE, Nittayajarn A, Merry J, Youngman P, Rubens CE. New genetic techniques for Group B Streptococci: High-efficiency transformation, maintenance of

568 temperature-sensitive pWV01 plasmids, and mutagenesis with Tn917. Applied and
569 Environmental Microbiology. 1997;63:3539-47.
570 45. Tan BK, Bogdanov M, Zhao J, Dowhan W, Raetz CRH, Guan Z. Discovery of a
571 cardiolipin synthase utilizing phosphatidylethanolamine and phosphatidylglycerol as
572 substrates. Proceedings of the National Academy of Sciences. 2012;109:16504-9.
573 46. Li C, Tan BK, Zhao J, Guan Z. In vivo and in vitro synthesis of
574 phosphatidylglycerol by an *Escherichia coli* cardiolipin synthase. Journal of Biological
575 Chemistry. 2016;291:25144-53.
576 47. Kim BJ, Hancock BM, Bermudez A, Del Cid N, Reyes E, van Sorge NM, et al.
577 Bacterial induction of Snail1 contributes to blood-brain barrier disruption. The Journal of
578 clinical investigation. 2015;125:2473-83.
579 48. Banerjee A, Kim BJ, Carmona EM, Cutting AS, Gurney MA, Carlos C, et al.
580 Bacterial Pili exploit integrin machinery to promote immune activation and efficient
581 blood-brain barrier penetration. Nature communications. 2011;2:462.

582

583

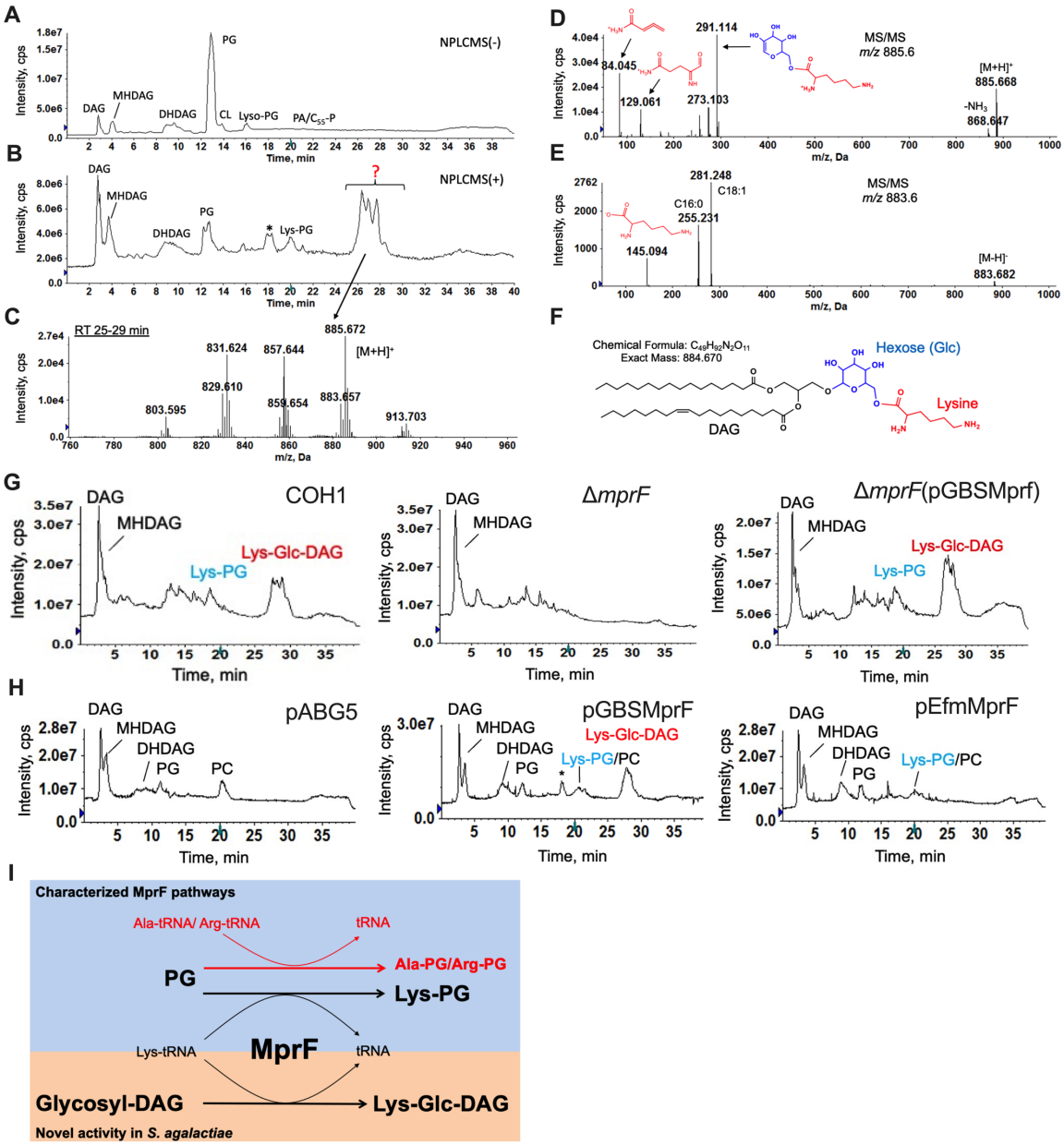

Fig 1. Lipidomic profiling of GBS and identification of Lys-Glc-DAG synthesized by MprF. Total ion chromatogram (TIC) of LC/MS in A) negative ion mode, B) positive ion mode shows a major unknown lipid eluting at ~25-29 min. C) Positive ESI/MS showing the $[M+H]^+$ ions of the unknown lipid. D) Positive ion MS/MS spectrum of $[M+H]^+$ at *m/z* 885.6 and E) negative ion MS/MS spectrum of $[M-H]^-$ at *m/z* 883.6 of the unknown lipid. F) Lys-Glc-DAG (16:0/18:1) is proposed as the structure of the unknown lipid. G) TIC showing loss of Lys-Glc-DAG and Lys-PG in COH1Δ*mprF* which is present when *mprF* is complemented *in trans*. H) Lys-Glc-DAG and Lys-PG is only present in *S. mitis* when expressing GBS *mprF* compared to Lys-PG only when expressing *E. faecium mprF*. "*" denotes methylcarbamate of Lys-Glc-DAG, an extraction artifact due to the use of chloroform. I) Biosynthetic pathways involving MprF.

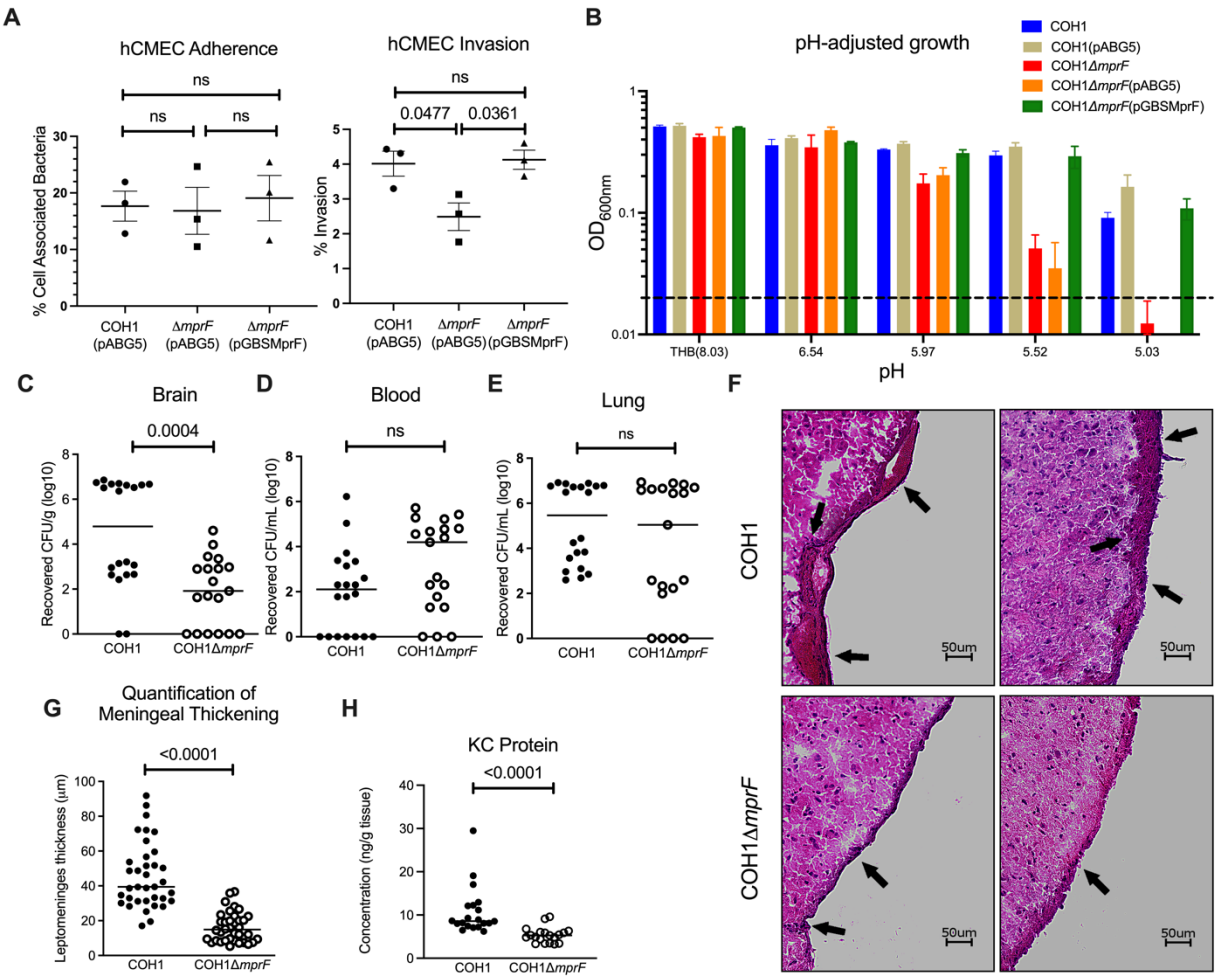

Fig 2. Contribution of lysine lipids to meningitis pathogenesis. A) *In vitro* assays for adherence and invasion of hCMEC cells indicates *mprF* contributes to invasion but not adherence to brain endothelium (the mean of each biological replicate is displayed, comprised of 4 replicate wells per biological replicate, mean and SEM). B) pH-adjusted medium growth indicates Δ*mprF* cannot survive in low pH conditions, mean and SD. Groups of CD-1 mice were injected intravenously with COH1 WT or COH1Δ*mprF* strains and bacterial counts were assessed in the C) brain, D) blood, and E) lung after 72h. Representative data from 2 independent experiments are shown (WT, *n* = 20; Δ*mprF, n* = 19). F) Hematoxylin-eosin-stained brain sections from representative mice infected with WT (top) or Δ*mprF* mutant (bottom); arrows indicate meningeal thickening and leukocyte infiltration. G) Quantification of meningeal thickening using ImageJ. H) KC chemokine production measured by ELISA. Panels C, D, E, G, and H) median indicated. Statistical analyses performed using GraphPad Prism: A) One-way ANOVA with Tukey's multiple comparisons test; C, D, F) unpaired two-tailed t-test; E, G) Mann-Whitney U test; p-values indicated; ns, no significance (p-value > 0.05).

Supplemental Figures, and Tables

Identification of a novel cationic glycolipid in *Streptococcus agalactiae* that contributes to brain entry and meningitis

Luke R. Joyce[a,b], Haider S. Manzer[b], Jéssica da C. Mendonça[b,c], Ricardo Villarreal[b], Prescilla E. Nagao[c] , Kelly S. Doran[b#,] Kelli L. Palmer[a#], and Ziqiang Guan[d#]

[a]Department of Biological Sciences, The University of Texas at Dallas, Richardson, TX, 75080

[b]Department of Immunology and Microbiology, University of Colorado School of Medicine, Aurora, CO, 80045

[c]Rio de Janeiro State University, Roberto Alcântara Gomes Biology Institute, Rio de Janeiro, RJ, Brazil

[d]Department of Biochemistry, Duke University Medical Center, Durham, NC, 27710

[#]Corresponding authors

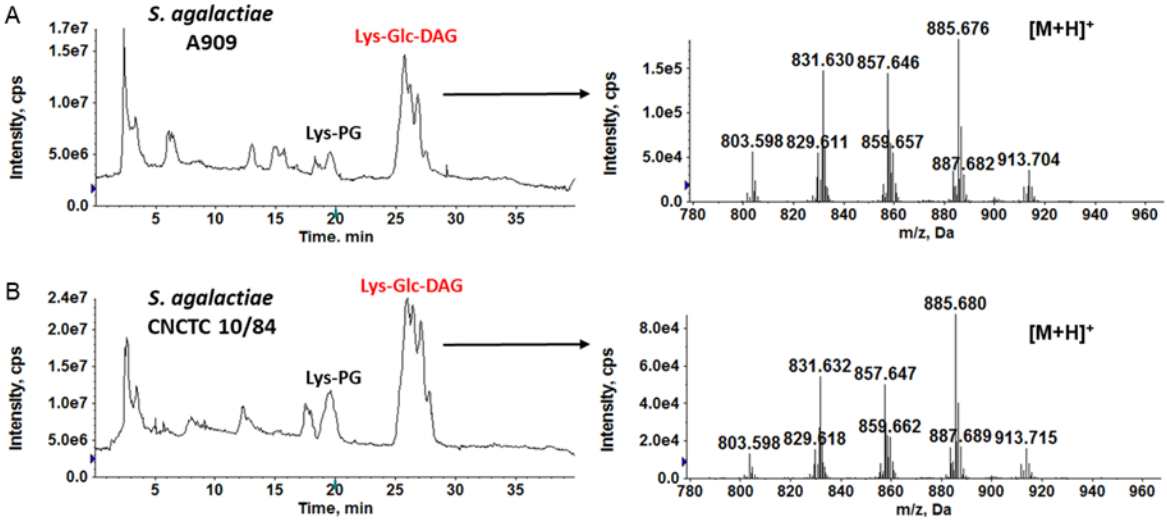

632

633 **S1 Fig. Detection of Lys-PG and Lys-Glc-DAG in *S. agalactiae* A909 and *S.***
634 ***agalactiae* CNCTC 10/84.** Positive TICs (left panels) showing the presence of Lys-PG
635 and Lys-Glc-DAG in S*. agalactiae* A909 and S*. agalactiae* CNCTC 10/84. Mass spectra
636 (right panels) show the $[M+H]^+$ ions of Lys-Glc-DAG.

637

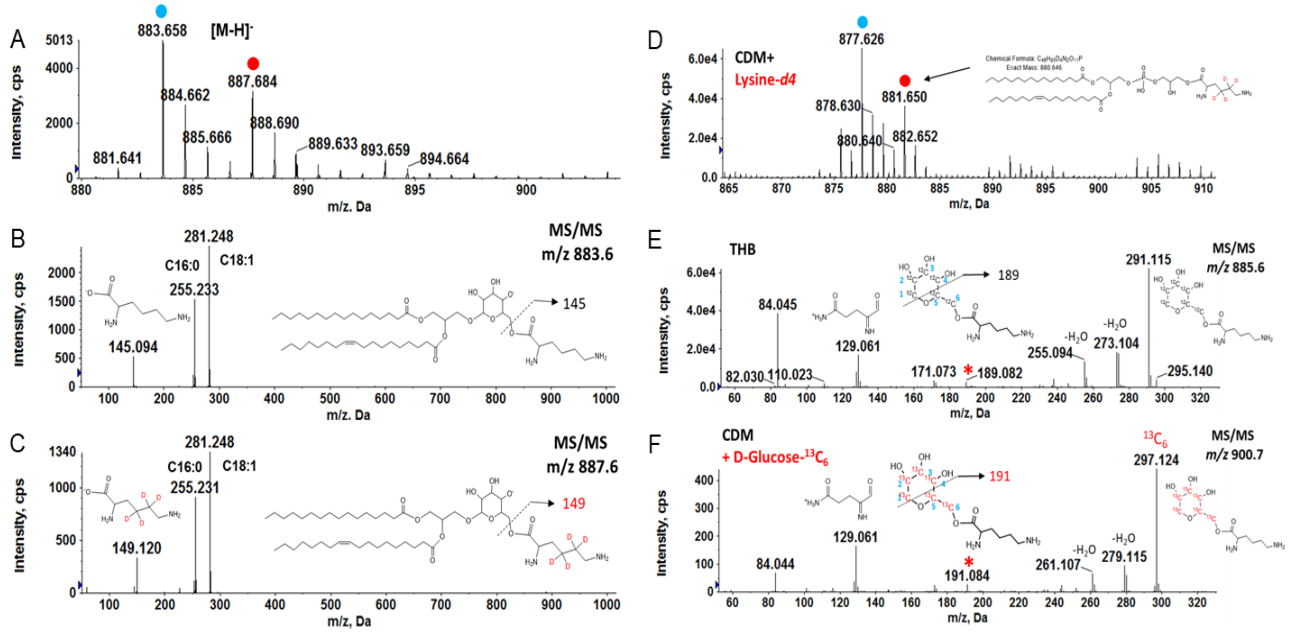

S2 Fig. Isotopic incorporation of deuterated lysine and ^{13}C-labeled glucose into Lys-Glc-DAG and Lys-PG. The lipid extracts of *S. agalactiae* COH1 cultured in DM, DM supplemented with 450 μM L-lysine-*d4* (4,4,5,5-D4), or in DM containing 0.5% w/v D-Glucose (U-$^{13}C_6$) were analyzed by LC-ESI/MS in the positive ion mode. A) Negative ESI/MS of $[M-H]^-$ ions of major Lys-Glc-DAG species in *S. agalactiae* COH1 when cultured in DM supplemented with lysine-*d4*. The incorporation of lysine-*d4* into Lys-Glc-DAG is evidenced by an upward *m/z* shift of 4 Da of the $[M-H]^-$ ion (from *m/z* 883 to *m/z* 887). B) MS/MS of $[M-H]^-$ at *m/z* 883.6 produces a deprotonated lysine residue at *m/z* 145. C) MS/MS of $[M-H]^-$ at *m/z* 887.6 produces a deprotonated lysine-*d4* residue at *m/z* 149. D) $[M+H]^+$ ions of major Lys-PG species in *S. agalactiae* COH1 cultured in DM supplemented with lysine-*d4.* The incorporation of lysine-*d4* in Lys-PG is evidenced by an upward *m/z* shift of 4 Da from unlabeled Lys-PG (blue dot) to labeled Lys-PG (red dot). E) MS/MS of 885.6. A major product ion at *m/z* 291.1 is derived from glucose-lysine residue. F) MS/MS of *m/z* 900.7 (containing fifteen ^{13}C atoms). The presence of *m/z* 297.1 (with 6 Da shift) is consistent with glucose in Lys-Glc-DAG is replaced with D-Glucose (U-$^{13}C_6$). The other nine ^{13}C atoms are incorporated into the DAG portion of Lys-Glc-DAG. Furthermore, MS/MS data indicate that lysine is linked to the C6 position of glucose by the fragmentation schemes for forming *m/z* 189 ion from the unlabeled Lys-Glc-DAG and *m/z* 191 ion from the ^{13}C-labeled Lys-Glc-DAG.

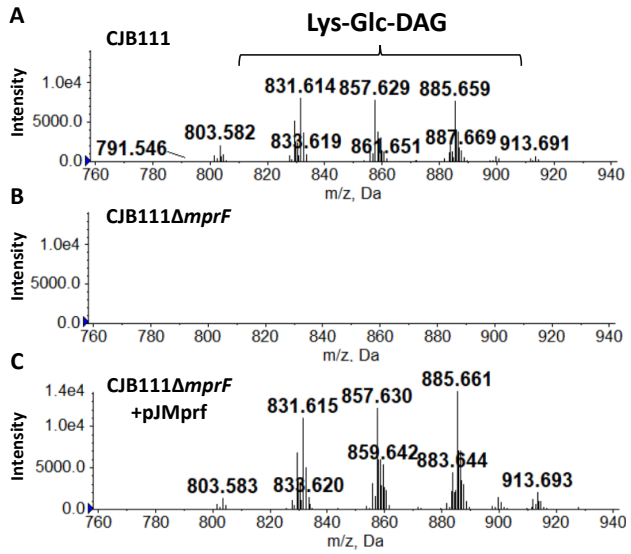

659

660 **S3 Fig. Positive ion mass spectra of retention time 27-29 minutes of hypervirulent**
661 **CJB111 strain.** Lys-Glc-DAG is present in the membrane of WT CJB111 (A). Deletion of
662 *mprF* from CJB111 genome results in loss of Lys-Glc-DAG from the membrane (B). *MprF*
663 complemented *in trans* reestablishes Lys-Glc-DAG back into the membrane (C).

664

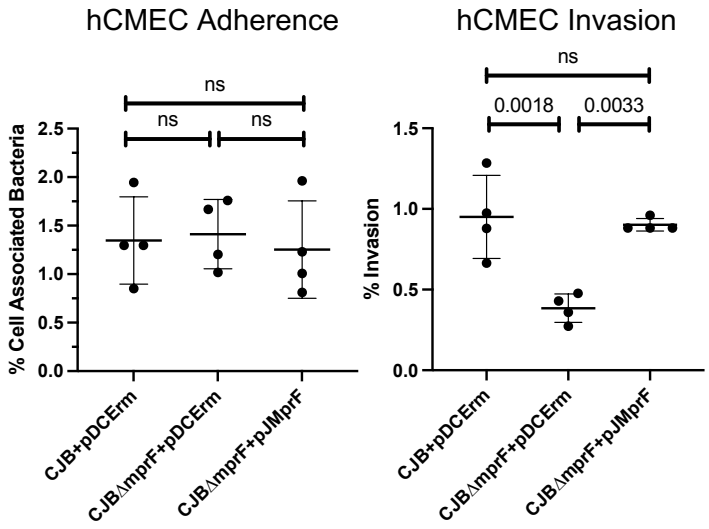

665

666 **S4 Fig. *In vitro* hCMEC adhesion and invasion of CJB111 strains**. *In vitro* assays for
667 adherence and invasion of hCMEC cells indicates *mprF* contributes to invasion but not
668 adherence to brain endothelium. Data indicates the percentage of the initial inoculum that
669 was recovered. Experiments were performed three times with each condition in
670 quadruplicate. Data from one representative experiment is shown, mean and standard
671 deviation indicated. One-Way ANOVA with Tukey's multiple comparisons statistical test
672 was used. P-values indicated; ns, not significant.

673 **S1 Table. Observed and calculated exact masses of the $[M+H]^+$ ions of Lys-Glc-**
674 **DAG molecular species in *S. agalactiae* COH1.**

Lys-Glc-DAG[1]	$[M+H]^+$	
	Observed mass	Exact mass
C28:1	801.575	801.583
C28:0	803.595	803.599
C30:1	829.610	829.615
C30:0	831.624	831.630
C32:2	855.623	855.630
C32:1	857.644	857.646
C34:2	883.657	883.622
C34:1	885.672	885.677
C36:2	911.686	911.693
C36:1	913.703	913.709

675

676 [1]The numbers before and after colons indicate the total acyl chain carbon atoms and
677 double bonds, respectively.

678 **S2 Table. Strains and plasmids used in this study.**

Organism	Strain	Description	Ref
S. agalactiae	ATCC BAA-1176 (COH1)	Wild-type *S. agalactiae* strain, serotype III	(1)
	COH1Δ*mprF*	*mprF* (GBSCOH1_1931) deletion strain	This work
	COH1Δ*mprF(*pABG5)	Empty vector control strain	This work
	COH1Δ*mprF*(pGBSMprf)	Expresses GBS *mprF* from P_{prtF} in pABG5Δ*phoZ*	This work
	COH1(pABG5)	Empty vector control	This work
	CJB111	Wilt-type *S. agalactiae* strain, serotype V	(2, 3)
	CJB111Δ*mprF*	*mprF* (ID870_10050) deletion strain	This work
	CJB111Δ*mprF*(pDCErm)	Empty vector control strain	This work
	CJB111Δ*mprF*(pJMprF)	Expresses GBS *mprF* in pDCErm	This work
	ATCC BAA-1138 (A909)	Wild-type *S. agalactiae* strain, serotype Ia	(4)
	CNCTC 10/84	Wild-type *S. agalactiae* strain, serotype V. Obtained from Dr. K Patras, UCSD	(5, 6)
S. mitis	ATCC 49456	Wild-type *S. mitis* type strain, also known as NCTC 12261	(7)
	ATCC 49456(pABG5)	Empty vector control	This work
	ATCC 49456(pGBSMprF)	Expresses GBS *mprF* from P_{prtF} in pABG5Δ*phoZ*	This work
	ATCC 49456(pEfmMprF)	Expresses *E. faecium mprF1* from P_{prtF} in pABG5Δ*phoZ*	This work
E. coli	DH5α	Plasmid cloning host; F^-, φ80*lacZ*ΔM15, *rec*A1, *end*A1, *hsd*R17, *pho*A, *sup*E44, λ^- *thi*-1, *gyr*A96, *rel*A1	(8)
	DH5α(pABG5)	Empty vector control	This work
	MC1061	Plasmid cloning host; F^-, araD139, Δ(araABC-leu)7696, Δ(lac)X74, galU, galK, hsdR2, (r_K^- m_K^+), mcrB1, rpsL, (Str^r)	(9)
	MC1061(pDCErm)	Empty vector control	This work
	DH5α(pGBSMprF)	Expresses COH1 *mprF* (GBSCOH1_1931) from P_{prtF} in pABG5Δ*phoZ*	This work

	DH5α(pEfmMprF)	Expresses *E. faecium mprF1* from P_{prtF} in pABG5Δ*phoZ*	This work
	DH5α(pMBMprFKO)	Allelic exchange plasmid containing ~2 kb sequence flanking GBSCOH1_1931	This work
	MC1061(pJMprFKO)	Allelic exchange plasmid containing ~2 kb sequence flanking ID870_10050	This work
	MC1061(pJMprF)	Expresses CJB11 *mprF* from $P_{tetM/erm}$ in pDCErm	This work
E. faecium	1,231,410	Wild type *E. faecium* strain	(10)

Plasmid	**Description**	**Ref**
pABG5Δ*phoZ*	Constitutive expression vector for streptococci with the P_{prtF} promoter. Confers kanamycin resistance. Referred to as pABG5 throughout the text	(11)
pGBSMprF	pABG5Δ*phoZ* expressing COH1 *mprF* (GBSCOH1_1931) from P_{prtF}	This work
pEfmMprF	pABG5Δ*phoZ* expressing *E. faecium* 1,231,410 *mprF1* (EFTG_00601) from P_{prtF}	This work
pMBSacB	Allelic exchange plasmid for *S. agalactiae*. Confers erythromycin resistance and sucrose sensitivity	(12)
pMBMprFKO	Knockout plasmid containing ~2 kb sequence flanking GBSCOH1_1931	This work
pJMprFKO	Knockout plasmid containing ~2 kb sequence flanking ID870_10050	This work
pDCErm	Consitituitive expression vector for streptococcus from $P_{tetM/erm}$	(13)
pJMprF	pDCErm expressing CJB111 *mprF* (ID870_10050)	This work

679

680

681 **S3 Table. Primers used in this study.**

Primer	5' – 3' sequence	Use
GBS_MprF_F	GAGAGGTCCCTTTCCTTGAAAAAGC TAATTGAAAAAGTC	Amplify GBSCOH1_1931 for Gibson assembly
GBS_MprF_R	ACCAATACCTTTATCTTATTTAACAA TCTTAATTTTACTATC	Amplify GBSCOH1_1931 for Gibson assembly
Faec_MprF1_F	GAGAGGTCCCTTTCCTTGTTAAAAA ATACCATACAATG	Amplify EFTG_00601 for Gibson assembly
Faec_MprF1_R	ACCAATACCTTTATCTTAATACTTTC TTCGTATCC	Amplify EFTG_00601 for Gibson assembly
MpF_SacII	ACGTCACCGCGGTTGAAAAAGCTAA TTGAAAAAGTC	Amplify CJB111 *mprF* ID870_10050 for ligation
MpR_BamHI	ACGTCAGGATCCTTATTTAACAATCT TAATTTTACTATC	Amplify CJB111 *mprF* ID870_10050 for ligation
pABG5-5'	GGAAAGGGACCTCTCTTCCTAAAC	Linearize pABG5Δ*phoZ* for Gibson assembly
pABG5-3'	GATAAAGGTATTGGTAAATAACAAA	Linearize pABG5Δ*phoZ* for Gibson assembly
	Expression plasmid sequencing	
GBS_S1	GAATGGAATAATATAGTAGGCT	For sequencing pGBSMprF/pJMprF, amplifies with pABG5_Fup2/ pF
GBS_S2	GATTGTATCCCTTATTCC	For sequencing pGBSMprF/pJMprF, amplifies with GBS_S3
GBS_S3	CGATTCAATAGCTTCAC	For sequencing pGBSMprF/pJMprF, amplifies with GBS_S2
GBS_S4	GATAAAAGGCTCTACTGG	For sequencing pGBSMprF/pJMprF, amplifies with pABG5_FDwn/pR
pABG5_FDwn	CCAATAATAATGACTAGAGAAG	For pABG5 plasmid insert sequencing
pABG5_Fup2	CAAAAGGTTTCGACTTTTCACC	For pABG5 plasmid insert sequencing
EF1_S1	GAATAACGCTGATCAAAAGT	For sequencing pEfmMprF1, amplifies with pABG5_Fup2
EF1_S2	TGCCAAGAGAAATAGTC	For sequencing pEfmMprF1, amplifies with EF1_S3
EF1_S3	ACAATCTCTTCGCTTG	For sequencing pEfmMprF1, amplifies with EF1_S2
EF1_S4	CCAACTGTTCTTCTCCAA	For sequencing pEfmMprF1, amplifies with pABG5_FDwn
pF	AGCGCTAGGAGGAAAC	For pDCErm plasmid insert sequencing
pR	CCCATGCCATCTCCAATC	For pDCErm plasmid insert sequencing
GBSCOH1_1931 knockout plasmid construction, sequencing, and integration screening		
Mp1F_PstI	ACGTCACTGCAGTTCAATTAGCTTTT TCAACAATTTC	Amplifies upstream fragment from within GBSCOH1_1931/ID870_10050 leaving 6 codons, with Mp1R_XhoI
Mp1R_XhoI	ACGTCACTCGAGGCTGTTTATGGTG CTTTG	5' most primer of upstream fragment, amplifies with Mp1F_PstI
Mp2F_XbaI	ACGTCATCTAGAGAAAAGGCTAGAT TACGAAC	3' most primer of downstream fragment, amplifies with Mp2R_PstI
Mp2R_PstI	ACGTCACTGCAGGTTAAATAAGCTTT ATTTGGCA	Amplifies downstream fragment leaving 2 codons and stop codon of GBSCOH1_1931/ID870_10050, with Mp2F_XbaI
T7 promoter	TAATACGACTCACTATAGGG	Amplifies with MpS5F below to sequence plasmid, amplifies with T3 promoter for insert screening and plasmid presence
T3 promoter	AATTAACCCTCACTAAAGGG	Amplifies with MpS3R below, amplifies with T7 promoter for insert screening and plasmid presence
Int_F	GCTAATTGAACTGCAGGTTAAATAA G	Anneals at *mprF* knockout site, amplifies with Out_R for single integration screening

Out_R	GCTATTATATTTAGTGGTTTAATTGG	Anneals outside recombination arms, amplifies with Int_F, for single integration screening
Genomic knockout region sequencing		
MpS3F	CATTAGCTAGTCTTATCGGAG	Anneals outside integration arms, amplifies with MpS3R
MpS3R	ACAGCTACTTGGTAGTTCA	Amplifies with MpS3F
MpS4F	GCTACTAAGGCAAGATACG	Amplifies with MpS4R, knockout screening and plasmid sequencing primer
MpS4R	ATGGTCAGCGATGGTG	Amplifies with MpS4F, knockout screening and plasmid sequencing primer
MpS5F	CATAAGCGAAATAACTTGAG	Amplifies with MpS5R
MpS5R	GTATACAACGGCTTGATTGG	Anneals outside integration arms, amplifies with MpS5F

682

683

References

1. Kuypers JM, Heggen LM, Rubens CE. Molecular analysis of a region of the Group B *Streptococcus* chromosome involved in type III capsule expression. Infection and immunity. 1989;57:3058-65.
2. Faralla C, Metruccio MM, De Chiara M, Mu R, Patras KA, Muzzi A, et al. Analysis of two-component systems in group B Streptococcus shows that RgfAC and the novel FspSR modulate virulence and bacterial fitness. mBio. 2014;5(3):e00870-14.
3. Spencer BL, Chatterjee A, Duerkop BA, Baker CJ, Doran KS. Complete Genome Sequence of Neonatal Clinical Group B Streptococcal Isolate CJB111. Microbiology resource announcements. 2021;10.
4. Lancefield RC, McCarty M, Everly WN. Multiple mouse-protective antibodies directed against Group B Streptococci. Special reference to antibodies effective against protein antigens. The Journal of experimental medicine. 1975;142:165-79.
5. Hooven TA, Randis TM, Daugherty SC, Narechania A, Planet PJ, Tettelin H, et al. Complete Genome Sequence of *Streptococcus agalactiae* CNCTC 10/84, a Hypervirulent Sequence Type 26 Strain. Genome announcements. 2014;2:e01338-14.
6. Wilkinson HW. Nontypable Group B Streptococci isolated from human sources. Journal of clinical microbiology. 1977;6:183-4.
7. Kilian M, Mikkelsen L, Henrichsen J. Taxonomic Study of Viridans Streptococci: Description of *Streptococcus gordonii* sp. nov. and Emended Descriptions of *Streptococcus sanguis* (White and Niven 1946), *Streptococcus oralis* (Bridge and Sneath 1982), and *Streptococcus mitis* (Andrewes and Horder 1906). International Journal of Systematic Bacteriology. 1989;39:471-84.
8. Taylor RG, Walker DC, Mclnnes RR. *E. coli* host strains significantly affect the quality of small scale plasmid DNA preparations used for sequencing. Nucleic acids research. 1993;21:1677-8.
9. Casadaban MJ, Cohen SN. Analysis of gene control signals by DNA fusion and cloning in Escherichia coli. J Mol Biol. 1980;138(2):179-207.
10. Palmer KL, Carniol K, Manson JM, Heiman D, Shea T, Young S, et al. High-quality draft genome sequences of 28 *Enterococcus* sp. isolates. Journal of bacteriology. 2010;192:2469-70.
11. Granok AB, Parsonage D, Ross RP, Caparon MG. The RofA binding site in *Streptococcus pyogenes* is utilized in multiple transcriptional pathways. Journal of bacteriology. 2000;182:1529-40.
12. Hooven TA, Bonakdar M, Chamby AB, Ratner AJ. A Counterselectable Sucrose Sensitivity Marker Permits Efficient and Flexible Mutagenesis in *Streptococcus agalactiae*. Applied and environmental microbiology. 2019;85:1-13.
13. Jeng A, Sakota V, Li Z, Datta V, Beall B, Nizet V. Molecular genetic analysis of a group A Streptococcus operon encoding serum opacity factor and a novel fibronectin-binding protein, SfbX. J Bacteriol. 2003;185(4):1208-17.